applied sciences

MDPI

Article

Loquat Leaf Extract Inhibits Oxidative Stress-Induced DNA Damage and Apoptosis via AMPK and Nrf2/HO-1 Signaling Pathways in C2C12 Cells

Young Hoon Kwon [1,†], Jung Yoon Jang [1,†], Jun Ho Lee [1], Young Whan Choi [2], Yung Hyun Choi [3] and Nam Deuk Kim [1,*]

[1] Department of Pharmacy, College of Pharmacy, Research Institute for Drug Development, Pusan National University, Busan 46241, Republic of Korea
[2] Department of Horticultural Bioscience, Pusan National University, Miryang 50463, Republic of Korea
[3] Department of Biochemistry, Dongeui University College of Korean Medicine, Busan 47340, Republic of Korea
* Correspondence: nadkim@pusan.ac.kr; Tel.: +82-51-510-2801; Fax: +82-51-513-6754
† These authors contributed equally to this work.

Abstract: Loquat (*Eriobotrya japonica*) leaf extract exhibits bioactive properties against a variety of diseases. However, it remains unclear whether loquat leaf extract can protect myoblasts from oxidative damage. To investigate the protective effect of loquat leaf ethanol extract (LE) against hydrogen peroxide (H_2O_2)-induced oxidative stress in C2C12 murine myoblasts and the effect of LE on cellular differentiation in C2C12 cells. LE inhibited H_2O_2-induced cytotoxicity and reduced both the expression level of γ-H2AX and reactive oxygen species formation. LE also inhibited H_2O_2-induced apoptosis, which resulted in the upregulation of B-cell lymphoma 2 and pro-caspase-3 and inhibition of poly(ADP-ribose) polymerase cleavage, and the dysfunction of mitochondria under H_2O_2-induced oxidative stress, which inhibited the release of cytochrome *c* from mitochondria to the cytoplasm. Moreover, LE upregulated p-AMP-activated protein kinase (AMPK), p-nuclear factor erythroid 2-related factor 2 (Nrf2), and heme oxygenase-1 (HO-1) and downregulated Kelch-like ECH-associated protein 1 in H_2O_2-treated C2C12 cells. In addition, LE promoted the differentiation of C2C12 cells into myotubes and increased the expression levels of myogenic proteins, myogenic differentiation 1 (MyoD) and myogenin. These findings suggest that LE may be a promising therapeutic candidate for treating oxidative stress-mediated myoblast injury and enhancing cellular differentiation of C2C12 murine myoblasts into myotubes.

Keywords: loquat leaf extract; reactive oxygen species; DNA damage; apoptosis; Nrf2/HO-1 signaling pathway; AMPK signaling pathway; differentiation

Citation: Kwon, Y.H.; Jang, J.Y.; Lee, J.H.; Choi, Y.W.; Choi, Y.H.; Kim, N.D. Loquat Leaf Extract Inhibits Oxidative Stress-Induced DNA Damage and Apoptosis via AMPK and Nrf2/HO-1 Signaling Pathways in C2C12 Cells. *Appl. Sci.* **2023**, *13*, 572. https://doi.org/10.3390/app13010572

Academic Editor: Francisco Arrebola

Received: 16 November 2022
Revised: 28 December 2022
Accepted: 30 December 2022
Published: 31 December 2022

1. Introduction

Oxidative stress, which results in the production of high levels of reactive oxygen species (ROS), is related to the onset of many chronic diseases. At low levels, these species function as second messengers in cell signaling and homeostasis, but the overproduction of ROS damages cellular biomolecules, such as proteins, lipids, and nucleic acids [1]. Mitochondria are important organelles that contribute to the generation of ROS within cells. ROS-mediated oxidative stress initiates the intrinsic apoptosis pathway, by inducing the release of cell death-promoting factors, including cytochrome *c* and caspase-9, from mitochondria into the cytoplasm [2]. Activated caspase-9 provokes the activation of effector caspases, such as caspase-3 and -7, which results in the degradation of various substrate proteins needed for cell survival; Bcl-2 family proteins play a vital role in this process [3]. Furthermore, mitochondrial dysfunction, due to inordinate ROS accumulation, may contribute to the activation of AMP-activated protein kinase (AMPK), a key sensor of energy

state, since it interrupts the efficient maintenance of energy supply and lowers intracellular ATP levels [4–6].

The formation of ROS occurs innately, and mammalian cells have developed a variety of mechanisms to limit ROS formation or detoxify ROS products. These mechanisms generally require antioxidant compounds and enzymes, including heme oxygenase-1 (HO-1), which is the rate-limiting inducible isoform protecting against oxidative stress [7]. The production of HO-1 is regulated by the nuclear factor-erythroid 2-related factor 2 (Nrf2)-antioxidant response element (ARE) pathway, and induction of the pathway protects cells against oxidative stress-induced cell death and tissue damage. Antioxidants are important substances that can protect cells from damage caused by ROS-mediated oxidative stress [8]. Thus, many researchers are searching for natural antioxidants with low cytotoxicity, safe and effective pharmacological activity, and the ability to prevent oxidative stress-mediated cell damage.

Eriobotrya japonica, also known as loquat, is a subtropical evergreen fruit tree native to China, where it has been cultivated for over 2000 years; the tree is now commercially grown in over 30 countries, including Pakistan, Israel, Republic of Korea, Japan, Turkey, India, Brazil, Spain, and Italy [9]. The seeds, leaves, and fruits of loquat tree are used extensively in food, tea, and traditional medicine. Previous research has demonstrated that loquat extracts contain a variety of antioxidants and exhibit bioactive properties that can counteract health problems, including cancer, diabetes, inflammation, bacterial and parasitic infections, pain, and allergies [10]. However, the mechanisms by which loquat extracts defend cells against oxidative stress-induced apoptosis remain unclear. Therefore, the goals of the present study were to investigate the ability of an ethanolic extract of loquat leaf to protect C2C12 murine myoblasts against cellular damage caused by hydrogen peroxide (H_2O_2) and to determine the mechanism(s) underlying this protective effect. In addition, the ability of loquat leaf ethanol extracts to induce differentiation of myoblasts into myotubes was investigated in C2C12 murine myoblasts.

2. Materials and Methods

2.1. Plant Material

Whole loquat leaves were collected and provided by PUREMIND (Yeongcheon, Republic of Korea) in October 2020 and authenticated by Young Whan Choi (Ph.D. in Medicinal Plants, Department of Horticultural Bioscience, College of Natural Resources & Life Science, Pusan National University, Miryang, Republic of Korea). A voucher specimen (PNU-0038) was deposited at College of Pharmacy, Pusan National University, Busan, Republic of Korea.

2.2. Chemicals and Reagents

All chemical reagents were purchased from Sigma-Aldrich (St. Louis, MO, USA) unless otherwise noted. Dulbecco's modified Eagle's medium (DMEM), fetal bovine serum (FBS), and penicillin-streptomycin were purchased from WelGENE (Gyeongsan, Republic of Korea), and horse serum was purchased from Invitrogen (Grand Island, NY, USA). Hydrogen peroxide (H_2O_2), 3-(4,5-dimethylthiazol-2-yl)-2,5-diphenyltetrazolium bromide (MTT), 4′,6-diamidino-2-phenylindole (DAPI), propidium iodide (PI), and 5,5′,6,6′-tetrachloro-1,1′,3,3′-tetraethyl-benzimidazolylcarbocyanine iodide (JC-1) were purchased from Sigma-Aldrich. The Annexin V-FITC Apoptosis Detection Kit and 2′,7′-dichlorofluorescein diacetate (DCF-DA) were purchased from R&D Systems Inc. (Minneapolis, MN, USA) and Molecular Probes, Inc. (Eugene, OR, USA), respectively. Antibodies against H2A histone family member X (H2AX, #2595), phosphorylated (p-) H2AX (γ-H2AX, Ser139, #2577), and p-AMPKα (Thr172, #2535), acetyl-CoA carboxylase (ACC, #3662), and p-ACC (Ser79, #3661) were purchased from Cell Signaling Technology, Inc. (Danvers, MA, USA). β-actin (sc-47778), Bcl-2 (B-cell lymphoma 2, sc-492), Bcl-2-associated X protein (Bax, sc-70405), pro-caspase-3 (sc-7272), poly(ADP-ribose) polymerase (PARP, sc-8007), cytochrome *c* (sc-13560), AMPKα1/2 (sc-74461), Nrf2 (sc-722), Kelch-like ECH-associated protein 1 (Keap1, sc-15246), HO-1 (sc-390991), myogenic differentiation 1 (MyoD, sc-304), and myogenin

(sc-52903) were obtained from Santa Cruz Biotechnology, Inc. (Dallas, TX, USA), and cytochrome *c* oxidase subunit IV (COX IV, ab14744) and p-Nrf2 (Ser40, ab180844) were purchased from Abcam, Inc. (Cambridge, MA, USA).

2.3. Preparation of the Loquat Extract (LE)

Briefly, the dried leaves (100 g) were ground and extracted twice using 70% ethanol at 70 °C (3 h each), after which the extraction mixture was filtered, and then the solvent was evaporated. The remaining extractant was dissolved in 150 mL 99% ethanol, mixed with 300 mL distilled water and incubated overnight at 4 °C to form a precipitate. After removing the supernatant, the remaining precipitate was washed twice with 33.3% ethanol, filtered, and dried on filter paper. The final amount of dried LE obtained was 4.25 g and the extracts were dissolved in dimethyl sulfoxide (DMSO) and stored at −20 °C until use. Control cells in all experiments were treated with DMSO as vehicle control and the maximum concentration of DMSO did not exceed 0.1% (*v*/*v*) in the range of treatments that did not affect cell growth.

2.4. Cell Culture and Viability Assays

For all experiments, C2C12 murine myoblasts (American Type Culture Collection, Manassas, VA, USA) were cultured to 70–80% confluence in growth medium that contained DMEM supplemented with 10% FBS, 100 U/mL penicillin, and 100 μg/mL streptomycin and were maintained under controlled conditions (95% relative humidity, 5% CO2, 37 °C).

When the cells reached 80–90% confluence, differentiation was induced by removing the growth medium, washing the cells with Dulbecco's phosphate-buffered saline, and then culturing the cells in differentiation medium that contained DMEM supplemented with 2% horse serum. To investigate the effect of the loquat leaf extract on myogenic differentiation, LE was also included in the differentiation medium.

For cell viability measurement, cells were incubated in MTT (0.5 mg/mL) for 3 h, lysed using formazan-formed DMSO, and quantified using an enzyme-linked immunosorbent assay (ELISA) plate reader (MR-7000; Dynatech Laboratories, Chantilly, VA, USA) to measure optical density at 540 nm.

2.5. ROS Quantification

To measure ROS levels, cells were treated with the indicated concentrations of H_2O_2 or compound C for 1 h, or pretreated with LE and compound C for 1 h followed by additional treatment with H_2O_2 for 1 h. Thereafter, the medium was replaced with a 10 μM DCF-DA solution and incubated for 30 min in a dark place. After staining, ROS production levels were measured using an Accuri™ C6 flow cytometer (BD Sciences, Franklin Lakes, NJ, USA) at excitation/emission wavelengths of 488/530 nm (10,000 events per sample).

2.6. Comet Assay

Comet analysis was performed to detect the migrating DNA in single cells on the gel. Cells were suspended in 1% low-melting-point agarose and aliquoted onto glass microscope slides, which aligned and electrophoresed at 30 V (1 V/cm) and 300 mA for 20 min. Finally, the slides were washed using 0.4 M Tris (pH 7.5) at 4 °C, stained using 20 μg/mL PI, and photographed using a fluorescence microscope (Carl Zeiss AG, Oberkochen, Germany). The images were analyzed using OpenComet software v1.3.1 [11]. The degree of DNA damage was graded on a scale of 0–4 counting at least 30 cells in each image using the following criteria: no damage (<5%) scored 0; low damage (5–20%) scored 1; moderate damage (20–40%) scored 2; high damage (40–80%) scored 3; extreme damage (>80%) scored 4.

2.7. Western Blot Analysis

To extract whole cellular proteins, the cells were collected, washed twice with ice-cold phosphate-buffered saline (PBS), and then lysed using the cell lysis buffer [25 mM Tris-Cl (pH 7.5), 250 mM NaCl, 5 mM Na-ethylenediaminetetraacetic acid (EDTA), 1%

nonidet-P40, 1 mM phenylmethylsulfonyl fluoride, and 5 mM dithiothreitol] for 1 h. The mitochondrial and cytosolic proteins were prepared using a mitochondria fractionation kit, in accordance with the instructions of the manufacturer (Active Motif, Inc., Carlsbad, CA, USA). Protein concentration of each sample was measured using protein assay reagent (Bio-Rad, Hercules, CA, USA). Equal amounts of protein were boiled in 2× Laemmli sample buffer (Bio-Rad) for 5 min. The protein samples were separated using sodium dodecyl sulfate-polyacrylamide gel electrophoresis on acrylamide gel and transferred to polyvinylidene fluoride membranes (Schleicher & Schuell, Inc., Keene, NH, USA). The membranes were blocked using 5% non-fat dry milk in Tris-buffered saline with Tween-20 buffer (TBST; 20 mM Tris, 100 mM NaCl, pH 7.5, and 0.1% Tween-20) for 1 h, incubated with primary antibodies at 4 °C overnight and washed three times using TBST buffer. Finally, the membranes were incubated with an HRP-conjugated secondary antibody (Santa Cruz Biotechnology) for 1 h at room temperature, and protein bands were detected using an enhanced chemiluminescent (ECL) detection system (R&D Systems) and a chemiluminescent imager (Azure Biosystems, Inc., Dublin, CA, USA).

2.8. Apoptosis Detection

The proportions of cells that had actively advanced to apoptosis were quantitatively measured using an Annexin V-FITC Apoptosis Detection Kit (BD Biosciences, San Jose, CA, USA). Briefly, the cells were treated with agents, harvested, treated with trypsin, washed using cold PBS, and resuspended in 1× binding buffer. The resulting aggregated cells were stained using PI and Annexin V-FITC solution at room temperature for 15 min in the dark and then analyzed by flow cytometry (BD Biosciences).

2.9. Nuclear Morphology Analysis

Chromatin condensation and nuclear fragmentation in the nuclei of apoptotic cells were evaluated using DAPI staining. Briefly, cells were harvested, washed twice using PBS, fixed using 3.7% paraformaldehyde in PBS at 25 °C for 10 min, washed using PBS, and stained using DAPI solution (1 mg/mL, 10 min). Finally, the stained cells were washed twice using PBS and examined under a fluorescence microscope (Carl Zeiss AG).

2.10. DNA Fragmentation Assays

Cells were incubated in lysis buffer [5 mM Tris-HCl (pH 7.5), 5 mM EDTA, and 0.5% Triton X-100] for 30 min on ice, and the resulting lysate was vortexed and centrifuged at 27,000 ×g for 20 min. The supernatant, which contained fragmented DNA, was treated with RNase and proteinase K, to degrade exogenous proteins, and then the fragmented DNA was extracted using a phenol/chloroform/isoamyl alcohol mixture (25:24:1, $v/v/v$) and precipitated using isopropanol. The resulting purified DNA was separated using electrophoresis on a 1.6% agarose gel, stained using 0.1 μg/mL EtBr, and visualized using a UV light source.

2.11. Measurement of Mitochondrial Membrane Potential (MMP)

To measure MMP ($\Delta\Psi m$), cells were harvested, washed using cold PBS, stained using a lipophilic cationic dye (JC-1, 10 μM, 20 min at 37 °C in the dark), washed using cold PBS, and then observed using flow cytometry.

2.12. Statistical Analysis

All experiments were performed independently at least three times. Data are expressed as mean ± standard deviation (SD) values and were analyzed using Prism (version 6.0; GraphPad Software, Inc., La Jolla, CA, USA). One-way ANOVA was used to determine the significance of group differences, and Tukey's post hoc test was used for pairwise comparisons. Statistical significance was set at $p < 0.05$.

3. Results

3.1. Effect of LE on Cytotoxicity of H_2O_2

Cytotoxicity of LE (0–20 μg/mL for 24 h) was assessed using the MTT assay, and no decrease in cell viability was observed up to 10 μg/mL LE (Figure 1a). To determine whether H_2O_2 is cytotoxic, C2C12 cells were treated with a broad range of H_2O_2 concentrations for 24 h, and then cell viability was investigated using the MTT assay. Cell viability was inhibited by H_2O_2-exposure in a concentration-dependent manner, and treatment with 0.6 and 0.8 mM H_2O_2 reduced cell viability to 67.2 and 63.3%, respectively (Figure 1b). Thus, 0.8 mM was selected as the optimal H_2O_2 concentration, and the maximum concentration of LE was selected as 10 μg/mL, so that the cytoprotective effect of LE against H_2O_2-induced cell damage and promotion of myogenic differentiation could be evaluated. In addition, pretreatment with 10 μg/mL LE prevented the loss of cell viability in H_2O_2-treated C2C12 cells by ~21% (Figure 1c). Furthermore, H_2O_2 treatment induced considerable morphological changes, including the development of irregular cell membrane buds and substantial vesicular vacuolization, which were effectively attenuated by LE pretreatment (Figure 1d). Thus, LE exposure exhibited protective activity against oxidative stress.

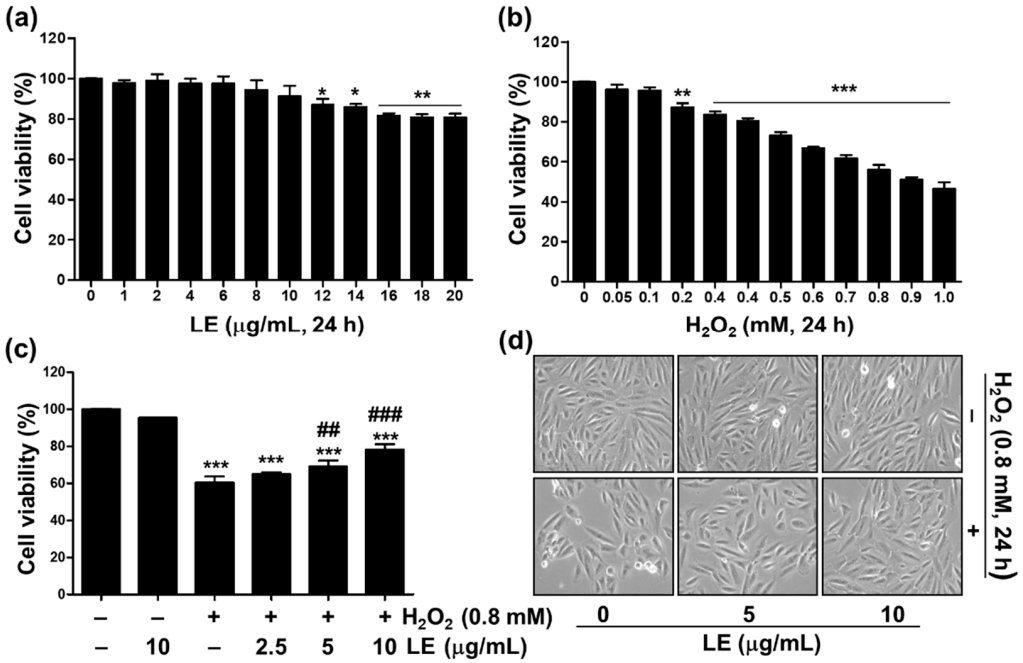

Figure 1. Effect of LE on H_2O_2-induced cytotoxicity in C2C12 cells. Cells were treated with various concentrations of LE (**a**) or H_2O_2 (**b**) for 24 h or pre-treated, with or without the indicated diverse concentrations of LE for 1 h prior to exposure to 0.8 mM H_2O_2 for 24 h (**c**,**d**); (**a**–**c**) Cell viability was assessed using a 3-(4,5-dimethylthiazol-2-yl)-2,5-diphenyltetrazolium bromide (MTT) assay. Data indicate mean ± SD values ($n = 3$; * $p < 0.05$, ** $p < 0.01$, and *** $p < 0.001$ vs. control cells; $^{\#\#}$ $p < 0.01$ and $^{\#\#\#}$ $p < 0.001$ vs. H_2O_2-treated cells); (**d**) Effect of LE on morphological changes in H_2O_2-treated cells. Representative results from three independent experiments are shown.

3.2. Effect of LE on ROS Generation and DNA Damage

The mechanism underlying the protective effect of LE against H_2O_2-induced cytotoxicity was evaluated. Levels of ROS were increased by 41.68% within 1 h of H_2O_2 treatment (Figure 2a) but were also 13.49% lower in cells pretreated with 10 μg/mL LE.

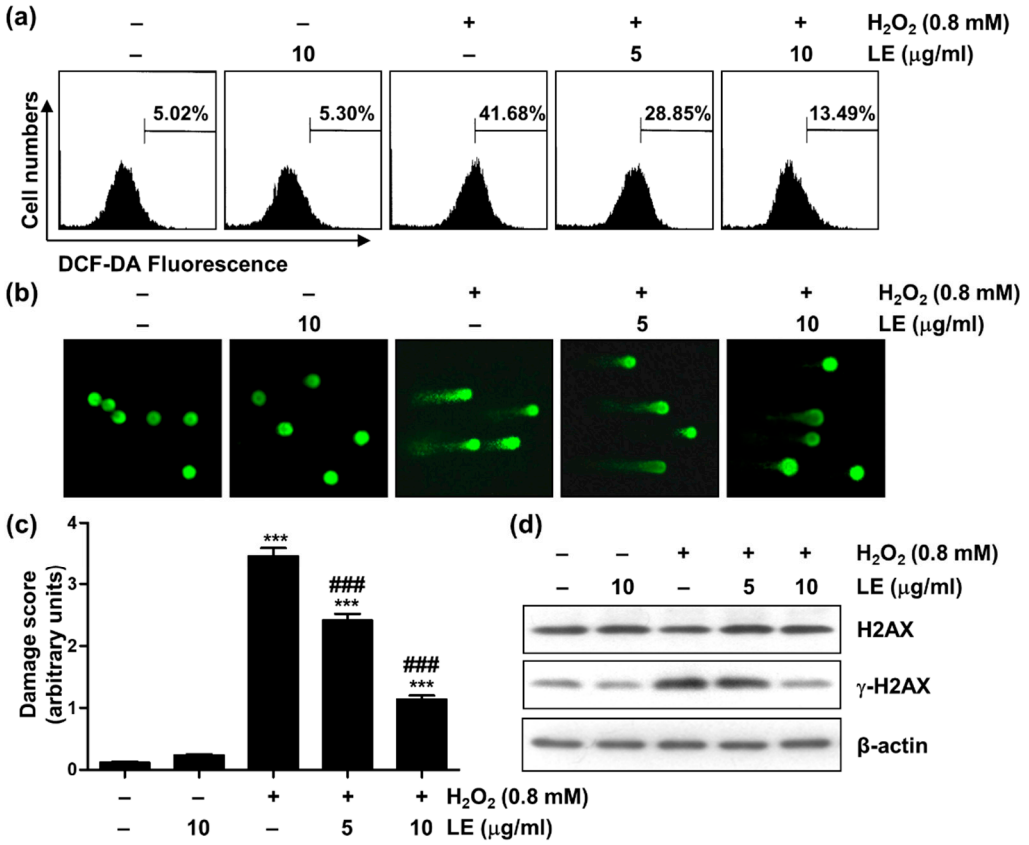

Figure 2. Effect of LE on H_2O_2-induced ROS generation and DNA damage in C2C12 cells. Cells were pretreated with LE for 1 h and treated, with or without 0.8 mM H_2O_2, for 1 h (**a**) or 24 h (**b**), (**c**), and (**d**). (**a**) Intracellular ROS levels were measured using 2′,7′-dichlorofluorescein diacetate (DCF-DA) staining and flow cytometry. Representative results of three independent experiments are shown; (**b**) DNA damage was evaluated using a comet assay. DNA damage is observed in the comet's tail, while intact DNA remains in the comet's head. Representative results of three independent experiments are shown; (**c**) DNA damage score. Data indicate mean ± SD values ($n = 3$; *** $p < 0.001$ vs. control cells; ### $p < 0.001$ vs. H_2O_2-treated cells); (**d**) H2AX and γ-H2AX levels analysis of cell lysates. Western blot analysis was performed using β-actin as a loading control. Representative results of three independent experiments are shown. H2AX, H2A histone family member X.

Next, the effect of LE on H_2O_2-mediated DNA damage was evaluated. Figure 2b shows the results of the comet assay conducted to assess the protective effect of LE against H_2O_2 induced DNA damage. In addition, the extents of DNA damage were manually measured and are shown in Figure 2c. Smear patterns of nuclear DNA were not observed in either the control cells or cells treated with 10 μg/mL LE alone (Figure 2b). However, because H_2O_2 compromised the integrity of the cell membrane, DNA was fragmented and observed as a comet-like structure outside the cell, and tail length was clearly increased in H_2O_2-treated cells. On the other hand, the tail length and smear pattern of H_2O_2-fragmented nuclear DNA were significantly shortened by pretreatment with 10 μg/mL LE. Meanwhile, the treatment of C2C12 cells with H_2O_2 did not significantly affect levels of H2AX, an important marker of DNA double-strand breaks [12], but increased H2AX phosphorylation levels at Ser139 (γH2AX). However, pretreatment with 10 μg/mL LE significantly reduced H_2O_2-induced γH2AX expression level (Figure 2d). Thus, LE reduced H_2O_2-induced ROS generation and DNA damage in C2C12 cells.

3.3. Effect of LE on Apoptosis

To determine whether the cytoprotective effect of LE on H_2O_2 was related to the inhibition of apoptosis, the effect of LE on the expression of apoptosis-related proteins

was evaluated by flow cytometry with Annexin V-FITC and PI double staining, DAPI staining, agarose gel electrophoresis analysis, and Western blot analysis. Annexin V-FITC and PI double staining indicated that H_2O_2 exposure increased apoptosis to 40.6%, whereas 10 μg/mL LE pretreatment reduced it to 9.41% (Figure 3a). Control cells had perfect nuclei, whereas H_2O_2-treated cells exhibited noticeable chromatin condensation (Figure 3b). However, such morphological changes were significantly reduced by 10 μg/mL LE pretreatment, and the concentration dependence of this effect was confirmed by agarose gel electrophoresis (Figure 3c).

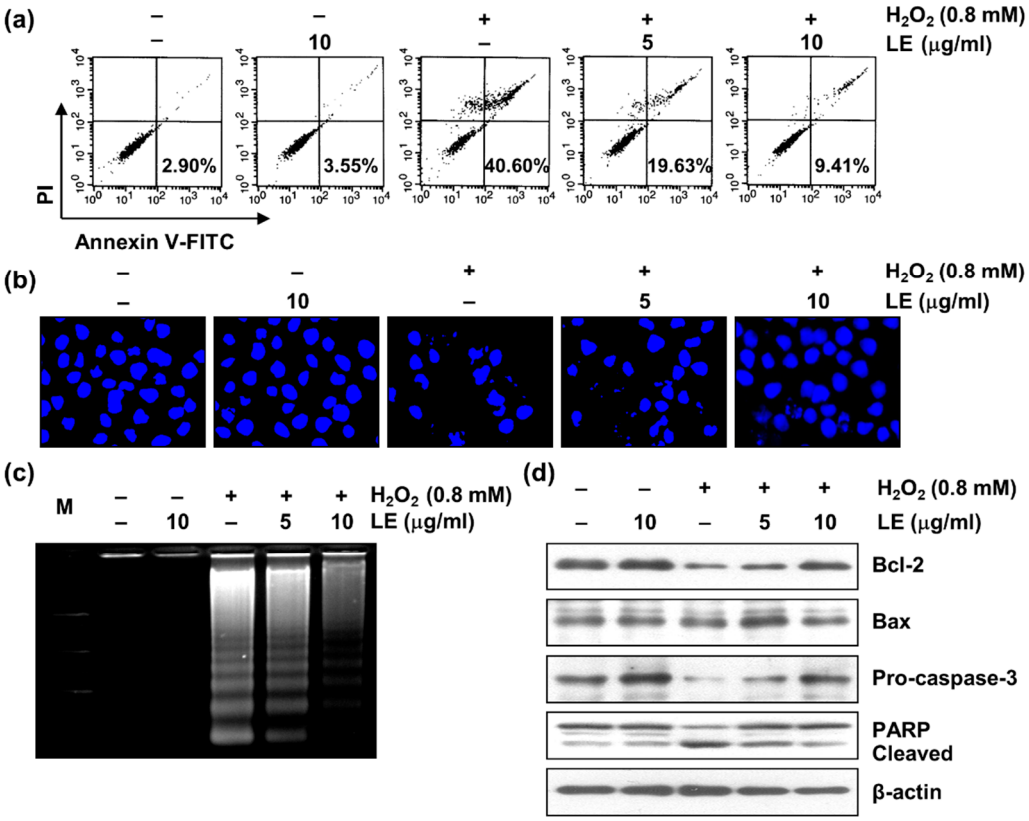

Figure 3. Effect of LE on H_2O_2-induced apoptosis in C2C12 cells. Cells were treated with LE for 1 h and then stimulated, with or without 0.8 mM H_2O_2, for 24 h: (**a**) The percentage of apoptotic cells was determined via Annexin V-FITC/PI assay. Representative results of three independent experiments are shown; (**b**) Cells were collected, fixed, and stained using 4′,6-diamidino-2-phenylindole (DAPI) solution. Stained nuclei (blue color) were observed using a fluorescence microscope. Representative results of three independent experiments are shown; (**c**) Assessment of genomic DNA fragmentation by agarose gel electrophoresis. M, Marker. Representative results of three independent experiments are shown; (**d**) Bcl-2, Bax, pro-caspase-3, and PARP levels in whole-cell lysates. Western blot analysis was performed using β-actin as a loading control. Representative results of three independent experiments are shown. Bcl-2, B-cell lymphoma 2; Bax, Bcl-2-associated X protein; PARP, poly(ADP-ribose) polymerase.

The mechanism underlying the anti-apoptotic effect of LE was then investigated by evaluating the effect of LE on H_2O_2-induced changes in the expression of apoptosis regulatory proteins. The expression levels of Bcl-2 and pro-caspase-3 were reduced by H_2O_2 treatment, whereas the level of cleaved PARP increased, and both changes were ameliorated by LE pretreatment, in a concentration-dependent manner (Figure 3d). However, Bax expression was not significantly affected by either H_2O_2 or LE pretreatment, which suggested that LE inhibited H_2O_2-induced apoptosis in C2C12 cells.

3.4. Effect of LE on Mitochondrial Dysfunction

To determine whether the suppression of mitochondrial damage was due to the cytoprotective effects of LE, MMP was measured using JC-1 staining. MMP was not affected by treatment with LE alone (Figure 4a,b) but was significantly reduced by with H_2O_2 treatment, and this reduction was ameliorated in the presence of LE (Figure 4a,b).

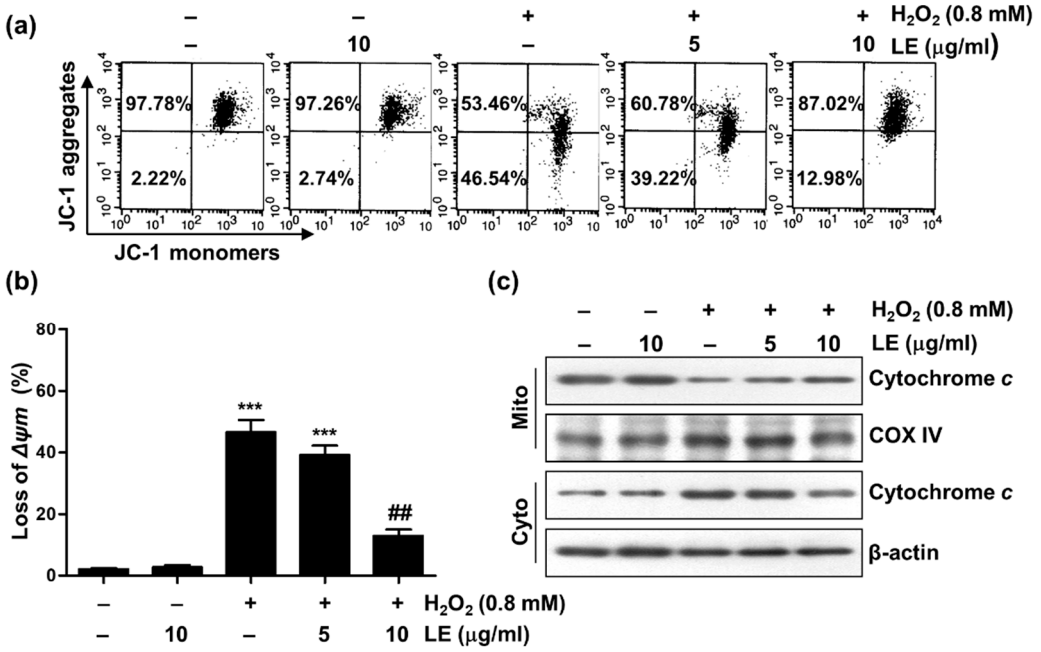

Figure 4. Effect of LE on H_2O_2-induced mitochondrial dysfunction in C2C12 cells. Cells were treated, with or without LE, for 1 h before treatment with 0.8 mM H_2O_2 for 24 h. (**a**) and (**b**) MMP was stained using 5,5′,6,6′-tetrachloro-1,1′,3,3′-tetraethyl-benzimidazolylcarbocyanine iodide (JC-1) and then analyzed using flow cytometry: (**a**) Typical results of three independent experiments of flow cytometry are shown; (**b**) Ratio of JC-1 aggregates to monomers. Data indicate mean ± SD values (n = 3; *** $p < 0.001$ vs. control cells; ## $p < 0.01$ vs. H_2O_2-treated cells); (**c**) Cytochrome *c* expression in mitochondrial and cytoplasmic fractions. Western blot analysis was performed using cytochrome *c* oxidase subunit IV (COX IV) and β-actin were as loading controls for mitochondria and cytoplasm, respectively. Representative results of three independent experiments are shown. Mito, mitochondrial fraction; Cyto, cytoplasmic fraction.

Because the release of cytochrome *c* from mitochondria is an important step in apoptosis [13], the effect of LE on changes in cytochrome *c* levels during the recovery process of H_2O_2-induced apoptosis was evaluated. The effect of H_2O_2 on the cytochrome *c* of cytoplasmic fractions suggested the release of cytochrome *c* from mitochondria, and these effects were ameliorated in LE-treated cells (Figure 4c). These results suggest that H_2O_2-induced apoptosis plays a significant role in mitochondrial dysfunction through MMP loss and that LE partially restores mitochondrial dysfunction.

3.5. Effect of LE on AMPK Signaling

Because previous studies have suggested that the AMPK pathway is activated by H_2O_2-induced oxidative stress in C2C12 murine myoblasts [14], the role of the AMPK signaling pathway in the cytotoxic protective effect of LE was evaluated. LE treatment did not affect AMPKα1/2 expression or acetyl-CoA carboxylase (ACC) levels but significantly increased p-AMPKα (Thr172) and p-ACC (Ser79) levels, in a concentration-dependent manner (Figure 5a). In addition, neither AMPKα1/2 nor p-AMPKα (Thr172) expression was affected by H_2O_2 treatment, and p-AMPKα (Thr172) expression, but not AMPKα1/2 expression, was upregulated by LE (Figure 5b).

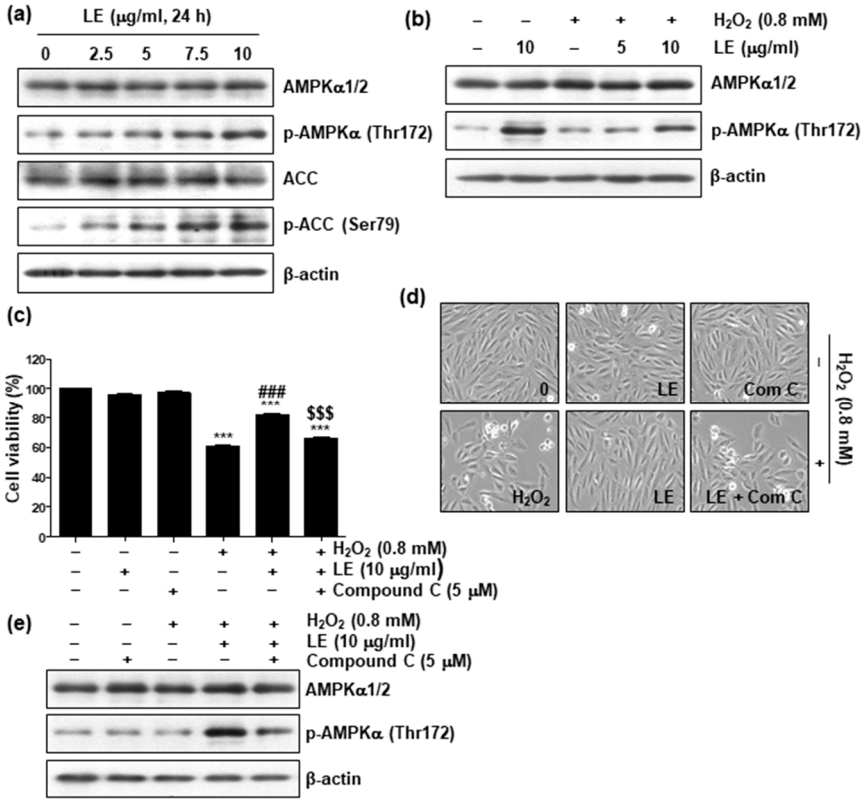

Figure 5. Effect of LE on AMPK signaling in C2C12 cells: (**a**) Effect of LE on the AMPKα1/2, p-AMPKα (Thr172), ACC, and p-ACC (Ser79) levels of total cell lysates. Western blot analysis was performed using β-actin as a loading control. Representative results from three independent experiments; (**b**) Effect of LE (1 h) and H_2O_2 (0.8 mM for 24 h) on AMPKα1/2 and p-AMPKα (Thr172) expression. Western blot analysis was performed using β-actin as a loading control. Representative results from three independent experiments; (**c**–**e**) Cells were pretreated using 5 μM compound C, with or without 10 μg/mL LE, for 1 h and then treated with 0.8 mM H_2O_2 for 24 h; (**c**) Cell viability was assessed using the MTT assay. Data indicate mean ± SD values (n = 3; *** $p < 0.001$ vs. control cells; ### $p < 0.001$ vs. H_2O_2-treated cells; $$$ $p < 0.001$ vs. H_2O_2 and LE treated cells); (**d**) Cell morphological changes. Representative results of three independent experiments, which were observed using phase-contrast microscopy, are shown; (**e**) AMPKα1/2 and p-AMPKα (Thr172) expression. Western blot analysis was performed using β-actin as a loading control. Representative results from three independent experiments are shown. AMPK, AMP-activated protein kinase; ACC, acetyl-CoA carboxylase; Com C, compound C.

Next, the AMPK inhibitor compound C was used to determine whether AMPK signaling was required for the protective effect of LE against H_2O_2-mediated cytotoxicity. The protective effects of LE against H_2O_2-induced growth inhibition and morphological changes were entirely abolished by compound C (Figure 5c,d). In addition, compound C significantly reduced the LE-mediated upregulation of p-AMPKα (Thr172) but had no significant effect on AMPKα1/2 expression. Thus, the protective activity of LE against oxidative damage involved the AMPK pathway (Figure 5e).

3.6. Effect of LE on AMPK-Dependent ROS Generation and DNA Damage

The effect of AMPK signaling on ROS generation was evaluated by pretreating cells with the AMPK inhibitor compound C. The H_2O_2-mediated increase in the DCF-DA staining cells (to 41.99%) was reduced (to 13.81%) by LE but restored (to 33.74%) by compound C (Figure 6a).

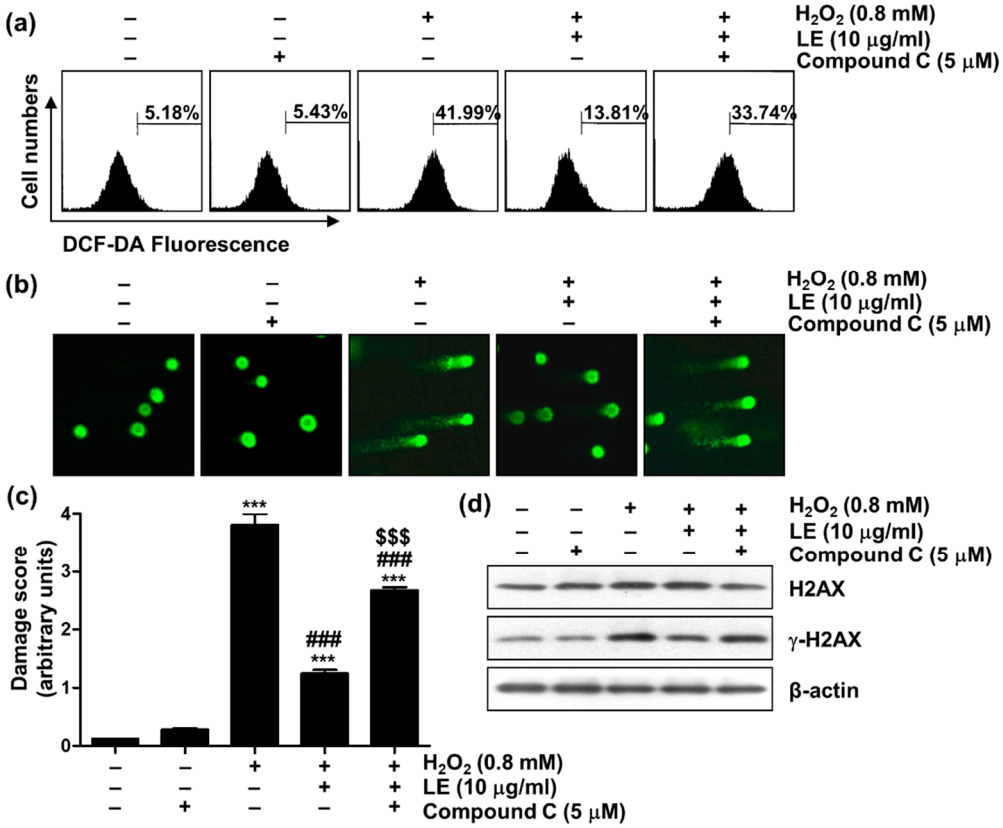

Figure 6. AMPK-dependent effect of LE on H_2O_2-induced ROS generation and DNA damage in C2C12 cells. Cells were pretreated using 5 μM compound C, with or without 10 μg/mL LE, for 1 h, followed by 0.8 mM H_2O_2 for 1 h (**a**) or 24 h (**b**–**d**). (**a**) After staining with DCF-DA, DCF fluorescence was measured using flow cytometry. Representative results of three independent experiments are shown; (**b**) DNA damage was measured using the comet assay. DNA damage is observed in the comet's tail, while intact DNA remains in the comet's head. Representative results of three independent experiments are shown; (**c**) DNA damage score. Data indicate mean ± SD values (n = 3; *** $p < 0.001$ vs. control cells; ### $p < 0.001$ vs. H_2O_2-treated cells; $$$ $p < 0.001$ vs. H_2O_2 and LE treated cells); (**d**) Cellular proteins were prepared and H2AX and γ-H2AX protein levels were analyzed. Western blot analysis was performed using β-actin as a loading control. Representative results of three independent experiments are shown. H2AX, H2A histone family member X.

The role of the AMPK pathway in the protective effects of LE against H_2O_2-induced DNA damage was investigated using comet analysis and the pretreatment of cells with the AMPK inhibitor compound C. DNA damage was clearly induced by H_2O_2 treatment (Figure 6b). The extents of DNA damage were manually measured and are shown in Figure 6c. However, DNA tails were not observed during the analysis of cells treated in the presence of LE, and this protective effect was attenuated by compound C. In addition, H2AX expression was not significantly affected by pretreatment with compound C (Figure 6d). However, γH2AX expression level was elevated by H_2O_2 treatment and reduced in the presence of LE, and the protective effect of LE against H_2O_2-induced DNA damage was attenuated by compound C. These results suggest that the AMPK-dependent protective effect of LE against H_2O_2-induced DNA damage is related to the inhibition of ROS generation.

3.7. Effect of LE on Nrf2/HO-1 Signaling

Because Nrf2 has been reported to play an important role in protection against oxidative stress through the ARE-mediated expression of phase II antioxidant enzymes [15], the role of the Nrf2/HO-1 pathway in the observed LE-induced antioxidant and cytoprotective

activities was investigated. LE treatment significantly enhanced the expression of HO-1, a target protein downstream of Nrf2, p-Nrf2 (Ser40), but not Nrf2, in a concentration-dependent manner, and decreased the expression of Keap1 [16], a negative regulator of Nrf2, in a concentration-dependent manner (Figure 7a).

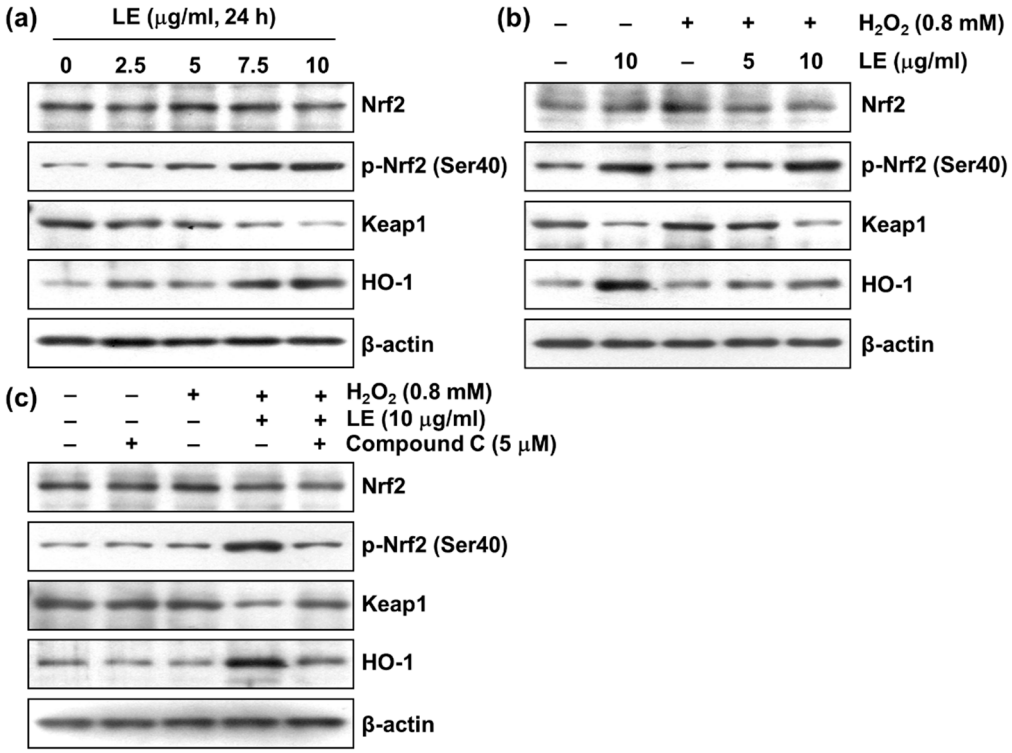

Figure 7. Effect of LE on Nrf2/HO-1 signaling in C2C12 cells: (**a**) Effect of LE on the Nrf2, p-Nrf2 (Ser40), Keap1, and HO-1 levels of total cell lysates. Western blot analysis was performed using β-actin as a loading control. Representative results of three independent experiments are shown; (**b**) Cells were pretreated with LE for 1 h and then stimulated in the presence or absence of 1 mM H_2O_2 for 24 h. Representative results of three independent experiments are shown. Cellular proteins were prepared and Nrf2, p-Nrf2 (Ser40), Keap1, and HO-1 protein levels analyzed. Western blot analysis was performed using β-actin as a loading control. Representative results from three independent experiments are shown; (**c**) Cells were pretreated with 5 μM compound C, with or without 10 μg/mL LE, for 1 h and then treated with 0.8 mM H_2O_2 for 24 h. Whole-cell lysates were prepared and Nrf2, p-Nrf2 (Ser40), Keap1, and HO-1 expression profiles were confirmed. Western blot analysis was performed using β-actin as a loading control. Representative results from three independent experiments are shown. Nrf2, nuclear factor erythroid 2-related factor 2; Keap1, Kelch-like ECH-associated protein 1; HO-1, heme oxygenase-1.

The expression level of Nrf2 was slightly elevated by H_2O_2 treatment but reduced when pretreated with LE (Figure 7b), whereas that of p-Nrf2 (Ser40) was unaffected by H_2O_2 treatment but increased when either treated with LE alone or pre-treated with LE. In contrast, Keap1 expression level was reduced by LE treatment and increased by H_2O_2 treatment, and the H_2O_2-mediated increase was significantly reduced by LE treatment. Meanwhile, HO-1 expression level was elevated by LE treatment, reduced by H_2O_2 treatment, and elevated in cells pretreated with LE.

Next, the effect of AMPK on the Nrf2/HO-1 signaling pathway in the protective effect of LE against H_2O_2-mediated cytotoxicity in C2C12 cells was investigated using the AMPK inhibitor compound C. The expression level of Nrf2 in C2C12 cells was slightly increased by H_2O_2 treatment but reduced with LE pretreatment and when treated with compound C (Figure 7c). The expression levels of p-Nrf2 (Ser40) and HO-1 were increased by H_2O_2 with LE pretreatment but reduced upon treatment with compound C. In addition, Keap1

expression level was reduced by H_2O_2 with LE pretreatment but increased upon treatment with compound C. These results suggest that LE activates the Nrf2/HO-1 signaling pathway and is affected by AMPK.

3.8. Role of AMPK in LE-Mediated Apoptosis Inhibition

The involvement of AMPK in the survival-improving effect of LE on H_2O_2-induced apoptosis in C2C12 cells was investigated. The formation of chromatin condensation in typical apoptotic cells was greatly increased by H_2O_2 treatment, and this effect was clearly ameliorated by LE. However, the protective effect of LE against H_2O_2-induced apoptosis was abolished by compound C (Figure 8a). Annexin V-positive cells, which represented the apoptotic population, was increased by H_2O_2 (to 41.28%) but reduced to 9.28% upon LE pretreatment. However, in the presence of compound C, the annexin V-positive cell population increased to 20.47% (Figure 8b). The induction of genomic DNA fragmentation by H_2O_2 treatment was reduced by pretreatment with LE but restored upon treatment with compound C (Figure 8c).

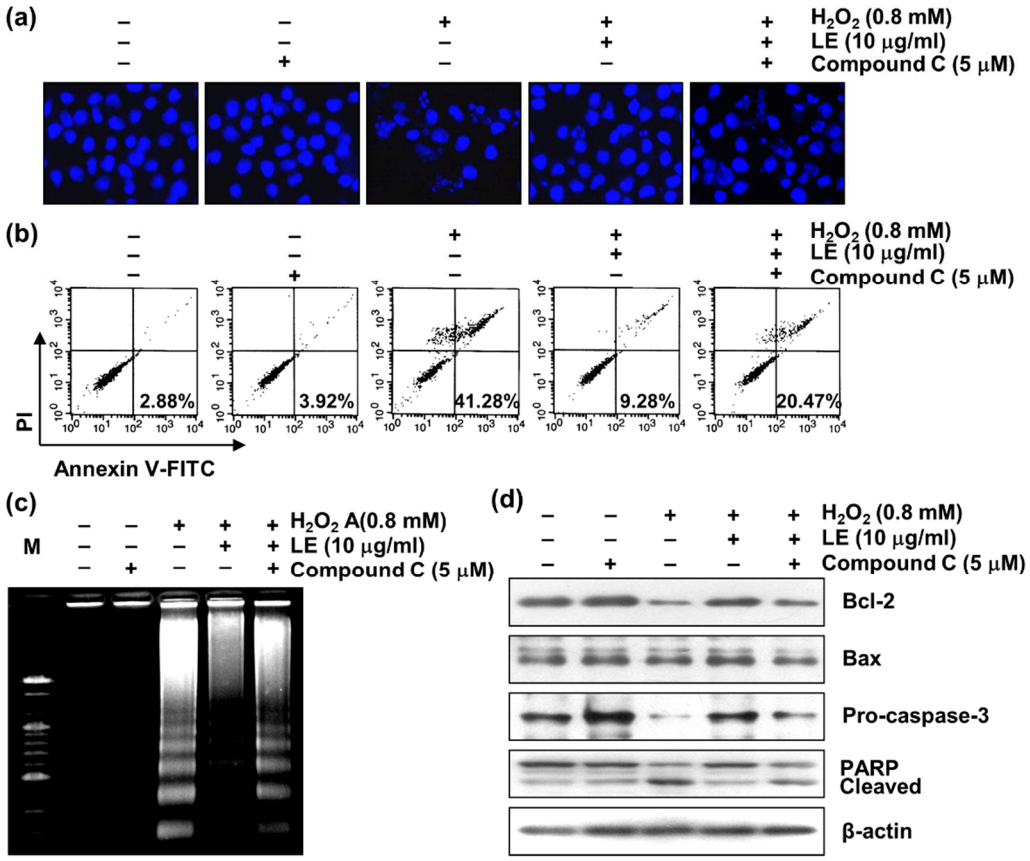

Figure 8. AMPK-dependent effect of LE on H_2O_2-induced apoptosis in C2C12 cells. Cells were pretreated with 5 μM compound C, with or without 10 μg/mL LE, for 1 h and then treated with 0.8 mM H_2O_2 for 24 h: (**a**) Induction of apoptosis was analyzed by measuring cells with condensed nuclei (blue color) later staining with 4′,6′-diamidino-2-phenylindole (DAPI) staining. Representative results of three independent experiments are shown; (**b**) Cells were stained using Annexin V-FITC/PI and then measured using flow cytometry. Representative results of three independent experiments are shown; (**c**) Fragmented genomic DNA was extracted from cells and measured using agarose gel electrophoresis. M, Marker. Representative results of three independent experiments are shown; (**d**) Expression profiles of Bcl-2, Bax, pro-caspase-3, and PARP proteins. Western blot analysis was performed using β-actin was as a loading control. Representative results of three independent experiments are shown. Bcl-2, B-cell lymphoma 2; Bax, Bcl-2-associated X protein; PARP, poly(ADP-ribose) polymerase.

Next, apoptosis-related marker proteins were analyzed by Western blotting. The expression levels of Bcl-2 and pro-caspase-3 were reduced by H_2O_2 treatment but increased with LE pretreatment, and the effects of LE pretreatment were attenuated by treatment with compound C (Figure 8d). In contrast, expression levels of Bax was relatively unaffected by treatment with H_2O_2, H_2O_2 with LE pretreatment, or compound C. In addition, the level of cleaved PARP was increased by H_2O_2 treatment, decreased with LE pretreatment, and increased by compound C. In summary, these results suggest that the protective effect of LE against oxidative stress-induced apoptosis involves AMPK signaling.

3.9. Role of AMPK in LE-Mediated Mitochondrial Dysfunction Inhibition

To investigate whether AMPK was involved in the suppressive effect of LE on H_2O_2-mediated mitochondrial dysfunction, the inhibitory effect of AMPK on the protective effect of LE against H_2O_2-induced MMP loss was evaluated. The H_2O_2-induced increase in impaired membrane potential was counteracted by treatment with LE, and the pretreatment of cells with compound C significantly increased membrane potential impairment (Figure 9a,b).

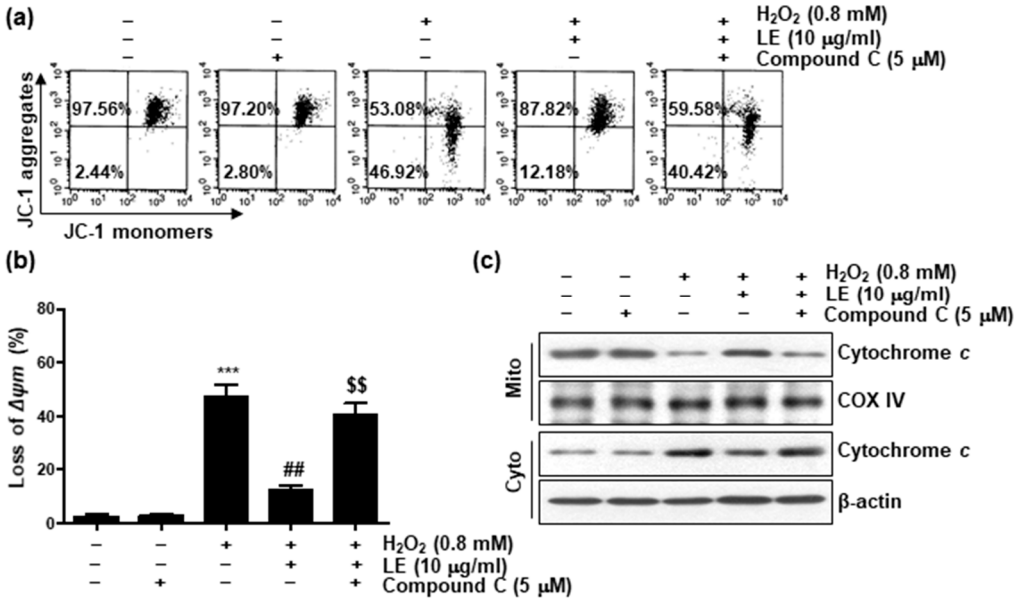

Figure 9. AMPK-dependent effect of LE on H_2O_2-induced mitochondrial dysfunction in C2C12 cells. Cells were pretreated with 5 μM compound C, with or without 10 μg/mL LE, for 1 h and then treated with 0.8 mM H_2O_2 for 24 h. (**a**), (**b**) MMP was measured using JC-1 staining and flow cytometry: (**a**) Representative results of flow cytometry analysis are shown; (**b**) The proportion of JC-1 aggregates to monomers. Data indicate mean ± SD values (n = 3; *** $p < 0.001$ vs. control cells; $^{\#\#}$ $p < 0.01$ vs. H_2O_2-treated cells, $^{\$\$}$ $p < 0.01$ vs. H_2O_2 and LE-treated cells); (**c**) Cytochrome *c* expression in mitochondrial and cytoplasmic fractions. Western blot analysis was performed using cytochrome *c* oxidase subunit IV (COX IV) and β-actin as internal controls for mitochondrial and cytoplasmic fractions, respectively. Representative results of three independent experiments are shown. Mito, mitochondrial fraction; Cyto, cytoplasmic fraction.

The results of Western blot analysis, using mitochondrial and cytoplasmic fractions, indicated that H_2O_2 increased the cytochrome *c* content of the cytoplasm and reduced that of mitochondria. In addition, these changes were significantly blocked by LE treatment, and the inhibitory effect of LE on cytochrome *c* leakage was abolished by compound C treatment (Figure 9c). These results suggest that LE contributes to the protection of mitochondrial function in H_2O_2-treated C2C12 cells by activating AMPK.

3.10. Effect of LE on Myotube Differentiation

The effect of LE on cellular differentiation was investigated using C2C12 myoblasts. Undifferentiated C2C12 cells were flat or star-shaped, whereas myotubes were fusiform, thick, and stretched in 3–4 directions (Figure 10a). On the third day of differentiation, myotube extension was promoted by LE treatment in a concentration-dependent manner. Next, myotube diameter was measured to determine the degree of differentiation. LE in C2C12 cells significantly increased the extent of differentiation in a concentration-dependent manner through the third day (Figure 10b).

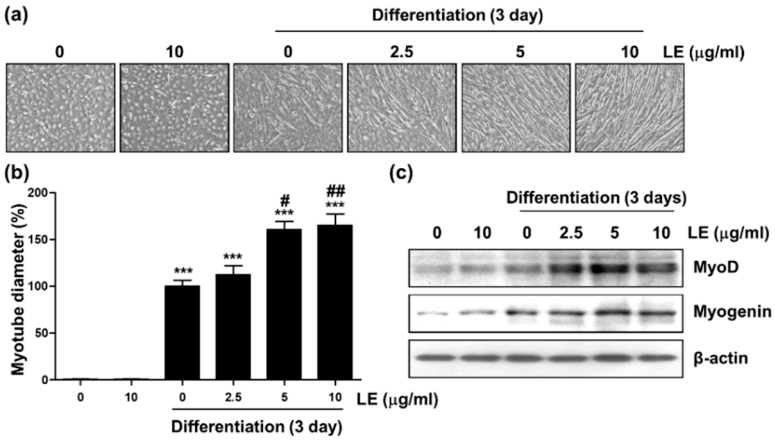

Figure 10. Effect of loquat leaf extract (LE) on C2C12 myoblast differentiation. The pre-differentiation step involved incubation for 2 days in differentiation medium that included 2% horse serum. Then, LE was added to the differentiation medium to induce myoblasts differentiation for 3 days: (**a**) Representative images of C2C12 cells. Cells were cultured for 3 days in differentiation medium, with or without LE. Representative results of three independent experiments are shown; (**b**) Effect of LE on myotube diameter after 3 days of differentiation. Data indicate mean ± SD values ($n = 3$; *** $p < 0.001$ vs. control cells; $^{\#}$ $p < 0.05$ and $^{\#\#}$ $p < 0.01$ vs. differentiated control cells); (**c**) Expression levels of MyoD and myogenin. Western blot analysis was performed using β-actin as a loading control. Representative results of three independent experiments are shown. MyoD, myogenic differentiation 1.

The mechanisms underlying the effect of LE on myogenic differentiation was investigated by monitoring myogenic regulatory factor (MRF) levels. LE treatment upregulated the expression of both MyoD and myogenin in a concentration-dependent manner (Figure 10c). These data suggest that LE induces the myogenic differentiation of C2C12 cells and this induction involves the upregulation of MyoD and myogenin.

4. Discussion

ROS can oxidize cellular components, thereby threatening cellular integrity. Some defense mechanisms protect cells from oxidative stress, and such mechanisms involve the clearance of specific proteins via the ubiquitin-proteasome system, upregulation of antioxidant production, and clearance of damaged organelles [17]. These defense systems are activated under excessive ROS conditions, leading to cell death via diverse signaling pathways and cascades [18]. Many previous studies have reported that natural compounds exhibit protective effects against oxidative stress. In addition, the inhibition of ROS production and accumulation by antioxidants may be effective in preventing oxidative DNA damage and cell death [19,20]. In the present study, the protective effect of LE against H_2O_2-induced oxidative stress and its mechanism was investigated in C2C12 cells. The results of this investigation indicate that LE can significantly reduce H_2O_2-induced DNA damage and apoptosis associated with the inhibition of ROS production (Figures 2 and 3).

The stress sensor AMPK can prevent ROS accumulation and alleviate oxidative stress [21] and also inhibits nicotinamide adenine dinucleotide phosphate consumption by phosphorylating ACC, which is a key downstream target. Therefore, AMPK is considered

a cell survival factor under conditions of oxidative stress [22,23]. Remarkably, the AMPK pathway shares noticeable crosstalk with antioxidant responses of Nrf2 [24]. Under normal physiological conditions, Nrf2 joins Keap1 in the cytoplasm, is ubiquitinated by the Cullin-3-Keap1 E3 ubiquitin ligase complex and is degraded through the ubiquitin proteasome pathway. When cells are exposed to oxidative stress, Nrf2 is released from Keap1 and migrates to the nucleus, where it promotes the transcriptional activation of ARE-responsive genes [25]. In the present study, LE activated AMPK and initiated AMPK under H_2O_2 stimulation conditions. However, the LE-mediated reversal of H_2O_2-induced cytotoxicity was eliminated by pretreatment with compound C, an AMPK inhibitor, which suggests that the activation of AMPK is involved in the protective effect of LE against oxidative stress-mediated cytotoxicity (Figure 5). As shown in Figure 7, LE treatment upregulated p-Nrf2 (Ser40) and HO-1 and downregulated Keap1, in a concentration-dependent manner. In addition, the expression levels of p-Nrf2 (Ser40) and HO-1 remarkably increased and the expression level of Keap1 noticeably diminished in the LE pretreatment group. However, these effects were completely abrogated by the AMPK inhibitor compound C, which suggested that LE activates the Nrf2/HO-1 signaling pathway and is affected by AMPK. In addition, the inhibitory effects of LE on H_2O_2-mediated ROS induction, DNA damage, and apoptosis were completely abolished by compound C. Together, these results suggest that LE protects against oxidative stress-induced cellular damage via AMPK activation (Figures 6 and 8).

Most C2C12 cells exposed to H_2O_2 undergo apoptosis accompanied by mitochondrial damage, and it is well known that apoptotic proteins, such as cytochrome *c*, are released into the cytoplasm during this process [26,27]. Cytoplasmic release of these proteins initiate the intrinsic apoptotic pathway and is controlled by members of the Bcl-2 family, which is composed of anti-apoptotic and pro-apoptotic proteins [28,29]. Bcl-2 proteins control the permeability of the mitochondrial outer membrane, thereby regulating the release of cytochrome *c* into the cytoplasm [29,30]. Therefore, to assess the inhibitory effect of LE on mitochondrial dysfunction, MMP and cytochrome *c* levels were evaluated. The results show that the loss of MMP and cytoplasmic cytochrome *c* level were significantly increased in H_2O_2-treated cells (Figure 4). However, LE pretreatment inhibited MMP reduction and increased mitochondrial cytochrome *c* levels, which indicated that LE can prevent oxidative stress-induced mitochondrial damage. Moreover, the reduction of anti-apoptotic protein Bcl-2 level by H_2O_2 was reversed by LE pretreatment, likely by blocking caspase-3 activity, thereby inhibiting the degradation of substrate proteins, like PARP (Figure 3d). However, the inhibitory effect of LE on H_2O_2-mediated mitochondrial dysfunction was abrogated by compound C (Figure 9).

According to previous studies, antioxidant and anti-inflammatory effects of LE have been reported [31,32]. In addition, several studies have reported that muscle cell differentiation including C2C12 cells is induced through antioxidant activity [14,33,34]. Therefore, we additionally studied the effect of LE on C2C12 cell differentiation along with the study of the mechanism, which is a major topic of apoptosis. The process of skeletal muscle creation (i.e., myogenesis [35]) is a basic physiological process related to muscle growth and regeneration [36]. MRF factors, such as MyoD, myogenic factor 5 (Myf5), myogenin, and myogenic regulatory factor 4 (MRF4) regulate the myogenic differentiation of the muscle lineage at multiple points and, thus, regulate the determination and differentiation of skeletal muscle cells during embryogenesis and postnatal myogenesis [37]. The findings of the present study indicate that LE promotes cell elongation and that the diameter of the resulting myotubes increased in a concentration-dependent manner, as did MyoD and myogenin expression levels (Figure 10). As myogenesis progresses, MRF family gene expression levels are greatly increased [38]. High levels of Myf5 expression result in the formation of primitive muscle structures, including committed muscle cells [39], and subsequent MyoD gene expression is initiated in the dermomyotome [37,40]. Two of these elements are muscle-determining genes and key factors in the activation of myogenic programs in both muscle and non-muscle cells [41]. Unlike MyoD and Myf5, myogenin is the main

regulator of muscle differentiation initiation, as demonstrated by the lower number of skeletal muscle fibers in myogenin-deficient mice [42]. The role of MRF4 is more complex during myogenesis. In mice, MRF4 is closely linked to the Myf5 gene, initiated in myotomes after Myf5 expression, and upregulated at the differentiated myocyte stage.

LE has been reported to contain ursolic acid (UA) as its main active ingredient [43,44]. UA was found to reduce muscle atrophy and stimulate muscle hypertrophy in vivo study [45]. Moreover, another previous study revealed that the LE supplements inhibited dexamethasone-induced reduction of muscle strength in Sprague Dawley rats [46]. In addition, a randomized, double-blind, placebo-controlled trial of 54 healthy adults investigated the effect of LE on human strength and muscle, and found that female subjects in the LE group had significantly better right-hand grip strength than subjects in the control group [47]. Accordingly, those results suggest the possibility of using LE as a therapeutic agent for the prevention of skeletal muscle atrophy and sarcopenia. In the LE used in this experiment, the content of UA was 161.2 mg/g. Therefore, the results of these experiments are very likely to be the effect of UA, and we plan to investigate this part through additional experiments that directly compare the two materials of LE and UA in the future.

5. Conclusions

The present study demonstrates that LE can effectively prevent H_2O_2-induced oxidative stress, DNA damage, apoptosis, and mitochondrial dysfunction via antioxidant action in C2C12 murine myoblasts. These findings suggest that the mechanisms underlying the cytoprotective effects of LE involve the AMPK and Nrf2/HO-1 signaling pathways and that the inhibitory effect of LE on H_2O_2-mediated ROS induction, DNA damage, apoptosis, and mitochondrial dysfunction involve the AMPK signaling pathway. In addition, the findings of the present study also confirm that LE promotes the differentiation of C2C12 myoblasts into myotubes (Figure 11). These results implicate LE as an effective agent for the prevention and treatment of diseases caused by oxidative stress.

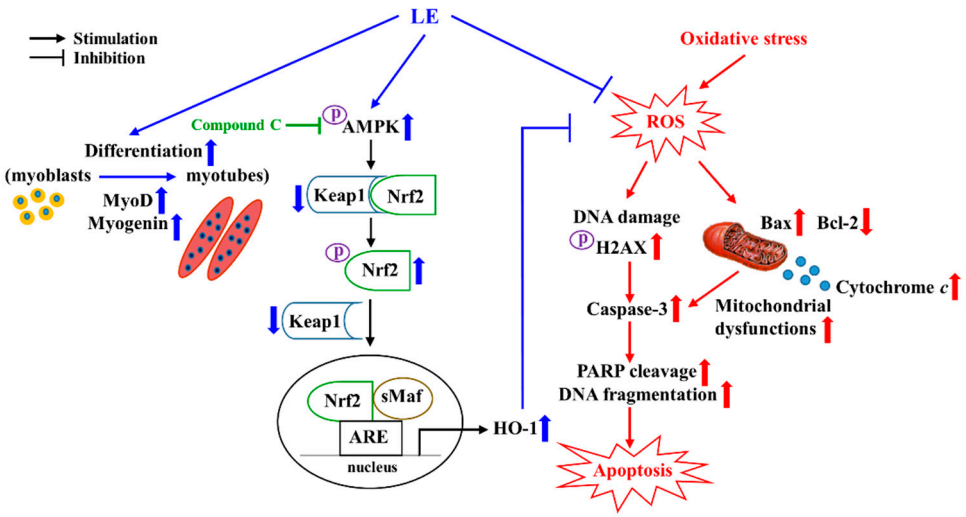

Figure 11. Schematic pathway of the effects of LE on oxidative stress-mediated DNA damage, apoptosis, and cell differentiation. AMPK, 5′ adenosine monophosphate-activated protein kinase; ARE, antioxidant response elements; Bax, Bcl-2 associated X protein; Bcl-2, B-cell lymphoma-2; Compound C, AMPK inhibitor; HO-1, heme oxygenase-1; H2AX, H2A histone family member X; Keap1, Kelch-like ECH-associated protein 1; MyoD, myogenic differentiation 1; Nrf2, nuclear factor erythroid 2-related factor 2; PARP, poly(ADP-ribose) polymerase; sMaf, small Maf.

Author Contributions: Writing—original draft preparation and formal analysis, Y.H.K. and J.Y.J.; data curation, J.H.L.; supervision, Y.W.C.; project administration, Y.H.C. and N.D.K.; funding acquisition, N.D.K. All authors have read and agreed to the published version of the manuscript.

Funding: This work was supported by BK21 FOUR Program by Pusan National University Research Grant, 2021 (Y.H.K.). This research was supported by Basic Science Research Program through the National Research Foundation of Korea (NRF) funded by the Ministry of Education (2022R1A6A3A01085858) (J.Y.J.). This study was supported by a National Research Foundation of Korea (NRF) grant funded by the Korean government (MSIT) (No. 2021R1F1A1051265) and the Basic Research Program through the National Research Foundation of Korea (NRF) funded by the Ministry of Education (2018R1D1A1B07044648) (N.D.K.).

Data Availability Statement: All data presented in this study are available on request from the corresponding author.

Conflicts of Interest: The authors declare no conflict of interest.

References

1. D'Autréaux, B.; Toledano, M.B. ROS as signalling molecules: Mechanisms that generate specificity in ROS homeostasis. *Nat. Rev. Mol. Cell Biol.* **2007**, *8*, 813–824. [CrossRef] [PubMed]
2. Wu, C.C.; Bratton, S.B. Regulation of the intrinsic apoptosis pathway by reactive oxygen species. *Antioxid. Redox Signal.* **2013**, *19*, 546–558. [CrossRef] [PubMed]
3. Kiraz, Y.; Adan, A.; Kartal Yandim, M.; Baran, Y. Major apoptotic mechanisms and genes involved in apoptosis. *Tumor Biol.* **2016**, *37*, 8471–8486. [CrossRef] [PubMed]
4. Zhao, Y.; Hu, X.; Liu, Y.; Dong, S.; Wen, Z.; He, W.; Zhang, S.; Huang, Q.; Shi, M. ROS signaling under metabolic stress: Cross-talk between AMPK and AKT pathway. *Mol. Cancer* **2017**, *16*, 79. [CrossRef] [PubMed]
5. Jeon, S.M. Regulation and function of AMPK in physiology and diseases. *Exp. Mol. Med.* **2016**, *48*, e245. [CrossRef]
6. Thirupathi, A.; de Souza, C.T. Multi-regulatory network of ROS: The interconnection of ROS, PGC-1 alpha, and AMPK-SIRT1 during exercise. *J. Physiol. Biochem.* **2017**, *73*, 487–494. [CrossRef]
7. Lee, E.K.; Kim, J.A.; Park, S.J.; Kim, J.K.; Heo, K.; Yang, K.M.; Son, T.G. Low-dose radiation activates Nrf1/2 through reactive species and the Ca^{2+}/ERK1/2 signaling pathway in human skin fibroblast cells. *BMB Rep.* **2013**, *46*, 258–263. [CrossRef]
8. Chapple, S.J.; Siow, R.C.; Mann, G.E. Crosstalk between Nrf2 and the proteasome: Therapeutic potential of Nrf2 inducers in vascular disease and aging. *Int. J. Biochem. Cell Biol.* **2012**, *44*, 1315–1320. [CrossRef]
9. Liu, Y.; Zhang, W.; Xu, C.; Li, X. Biological activities of extracts from loquat (*Eriobotrya japonica* Lindl.): A Review. *Int. J. Mol. Sci.* **2016**, *17*, 1983. [CrossRef]
10. Jabir, M.S.; Hussien, A.A.; Sulaiman, G.M.; Yaseen, N.Y.; Dewir, Y.H.; Alwahibi, M.S.; Soliman, D.A.; Rizwana, H. Green synthesis of silver nanoparticles from *Eriobotrya japonica* extract: A promising approach against cancer cells proliferation, inflammation, allergic disorders and phagocytosis induction. *Artif. Cells Nanomed. Biotechnol.* **2021**, *49*, 48–60. [CrossRef]
11. OpenComet Scoring Software, Version 1.3.1. Available online: http://cometbio.org (accessed on 27 December 2022).
12. Stope, M. Phosphorylation of histone H2A.X as a DNA-associated biomarker (Review). *World Acad. Sci. J.* **2021**, *3*, 31. [CrossRef]
13. Gogvadze, V.; Orrenius, S.; Zhivotovsky, B. Multiple pathways of cytochrome *c* release from mitochondria in apoptosis. *Biochim. Biophys. Acta* **2006**, *1757*, 639–647. [CrossRef] [PubMed]
14. Park, C.; Ji, S.Y.; Lee, H.; Choi, S.H.; Kwon, C.Y.; Kim, S.Y.; Lee, E.T.; Choo, S.T.; Kim, G.Y.; Choi, Y.H.; et al. *Mori ramulus* suppresses hydrogen peroxide-induced oxidative damage in murine myoblast C2C12 cells through activation of AMPK. *Int. J. Mol. Sci.* **2021**, *22*, 11729. [CrossRef]
15. Yuan, J.; Lu, Y.; Wang, H.; Feng, Y.; Jiang, S.; Gao, X.-H.; Qi, R.; Wu, Y.; Chen, H.-D. Paeoniflorin resists H_2O_2-induced oxidative stress in melanocytes by JNK/Nrf2/HO-1 pathway. *Front. Pharmacol.* **2020**, *11*, 536. [CrossRef] [PubMed]
16. Katsuragi, Y.; Ichimura, Y.; Komatsu, M. Regulation of the Keap1–Nrf2 pathway by p62/SQSTM1. *Curr. Opin. Toxicol.* **2016**, *1*, 54–61. [CrossRef]
17. Scherz-Shouval, R.; Elazar, Z. ROS, mitochondria and the regulation of autophagy. *Trends Cell Biol.* **2007**, *17*, 422–427. [CrossRef]
18. Kang, J.S.; Han, M.H.; Kim, G.Y.; Kim, C.M.; Kim, B.W.; Hwang, H.J.; Hyun, Y. Nrf2-mediated HO-1 induction contributes to antioxidant capacity of a Schisandrae Fructus ethanol extract in C2C12 myoblasts. *Nutrients* **2014**, *6*, 5667–5678. [CrossRef]
19. Rajendran, P.; Nandakumar, N.; Rengarajan, T.; Palaniswami, R.; Gnanadhas, E.N.; Lakshminarasaiah, U.; Gopas, J.; Nishigaki, I. Antioxidants and human diseases. *Clin. Chim. Acta* **2014**, *436*, 332–347. [CrossRef]
20. Yang, H.Y.; Lee, T.H. Antioxidant enzymes as redox-based biomarkers: A brief review. *BMB Rep.* **2015**, *48*, 200–208. [CrossRef]
21. Wang, S.; Song, P.; Zou, M.-H. AMP-activated protein kinase, stress responses and cardiovascular diseases. *Clin. Sci. (Lond.)* **2012**, *122*, 555–573. [CrossRef]
22. Zhao, Y.; Li, S.; Wang, X.; Wang, G.; Shi, M.; Wu, J. Design of a novel multi channel photonic crystal fiber polarization beam splitter. *Opt. Commun.* **2017**, *400*, 79–83. [CrossRef]

23. Cardaci, S.; Filomeni, G.; Ciriolo, M.R. Redox implications of AMPK-mediated signal transduction beyond energetic clues. *J. Cell Sci.* **2012**, *125*, 2115–2125. [CrossRef] [PubMed]
24. Mo, C.; Wang, L.; Zhang, J.; Numazawa, S.; Tang, H.; Tang, X.; Han, X.; Li, J.; Yang, M.; Wang, Z.; et al. The crosstalk between Nrf2 and AMPK signal pathways is important for the anti-inflammatory effect of berberine in LPS-stimulated macrophages and endotoxin-shocked mice. *Antioxid. Redox Signal.* **2014**, *20*, 574–588. [CrossRef] [PubMed]
25. Choi, Y.H. Activation of the Nrf2/HO-1 signaling pathway contributes to the protective effects of platycodin D against oxidative stress-induced DNA damage and apoptosis in C2C12 myoblasts. *Gen. Physiol. Biophys.* **2020**, *39*, 519–530. [CrossRef] [PubMed]
26. Siu, P.M.; Wang, Y.; Alway, S.E. Apoptotic signaling induced by H_2O_2-mediated oxidative stress in differentiated C2C12 myotubes. *Life Sci.* **2009**, *84*, 468–481. [CrossRef]
27. Choi, Y.H. Trans-cinnamaldehyde protects C2C12 myoblasts from DNA damage, mitochondrial dysfunction and apoptosis caused by oxidative stress through inhibiting ROS production. *Genes Genom.* **2021**, *43*, 303–312. [CrossRef]
28. Jakubczyk, K.; Dec, K.; Kałduńska, J.; Kawczuga, D.; Kochman, J.; Janda, K. Reactive oxygen species—Sources, functions, oxidative damage. *Pol. Merkur. Lekarski* **2020**, *48*, 124–127.
29. Dadsena, S.; King, L.E.; García-Sáez, A.J. Apoptosis regulation at the mitochondria membrane level. *Biochim. Biophys. Acta. Biomembr.* **2021**, *1863*, 183716. [CrossRef]
30. Xiong, S.; Mu, T.; Wang, G.; Jiang, X. Mitochondria-mediated apoptosis in mammals. *Protein Cell* **2014**, *5*, 737–749. [CrossRef]
31. Hasibuan, F.E.; Syahfitri, W.; Ilyas, S.; Hutahaean, S. Phytochemical screening, antioxidant activity and thin-layer chromatography test of methanol extract and simplicia leaves of loquat (*Eriobotrya japonica* Lindl). *IOP Conf. Ser. Mater. Sci. Eng.* **2020**, *725*, 012069. [CrossRef]
32. Hyun, M.K.; Kim, D.H.; Park, C.H.; Noh, S.G.; Choi, S.; Lee, J.Y.; Choi, J.H.; Park, D.; Choi, Y.J.; Chung, H.Y. Protective mechanisms of loquat leaf extract and ursolic acid against diabetic pro-inflammation. *J. Mol. Med.* **2022**, *100*, 1455–1464. [CrossRef] [PubMed]
33. Zhou, L.; Lu, R.; Huang, C.; Lin, D. Taurine Protects C2C12 Myoblasts from impaired cell proliferation and myotube differentiation under cisplatin-induced ROS exposure. *Front. Mol. Biosci.* **2021**, *8*, 685362. [CrossRef] [PubMed]
34. Lee, S.C.; Lee, N.H.; Patel, K.D.; Jun, S.K.; Park, J.H.; Knowles, J.C.; Kim, H.W.; Lee, H.H.; Lee, J.H. A Study on myogenesis by regulation of reactive oxygen species and cytotoxic activity by selenium nanoparticles. *Antioxidants* **2021**, *10*, 1727. [CrossRef] [PubMed]
35. Lin, M.; Zhou, S.; Sakamoto, K. Alpha Mangostin promotes myogenic differentiation of C2C12 mouse myoblast cells. *Biochem. Biophys. Res. Commun.* **2020**, *528*, 193–198. [CrossRef] [PubMed]
36. Meng, Z.X.; Li, S.; Wang, L.; Ko, H.J.; Lee, Y.; Jung, D.Y.; Okutsu, M.; Yan, Z.; Kim, J.K.; Lin, J.D. Baf60c drives glycolytic metabolism in the muscle and improves systemic glucose homeostasis through Deptor-mediated Akt activation. *Nat. Med.* **2013**, *19*, 640–645. [CrossRef] [PubMed]
37. Buckingham, M.; Rigby, P.W. Gene regulatory networks and transcriptional mechanisms that control myogenesis. *Dev. Cell* **2014**, *28*, 225–238. [CrossRef] [PubMed]
38. Yusuf, F.; Brand-Saberi, B. The eventful somite: Patterning, fate determination and cell division in the somite. *Anat. Embryol.* **2006**, *211* (Suppl. 1), 21–30. [CrossRef] [PubMed]
39. Bentzinger, C.F.; Wang, Y.X.; Rudnicki, M.A. Building muscle: Molecular regulation of myogenesis. *Cold Spring Harb. Perspect. Biol.* **2012**, *4*, a008342. [CrossRef]
40. Yokoyama, S.; Asahara, H. The myogenic transcriptional network. *Cell. Mol. Life Sci.* **2011**, *68*, 1843–1849. [CrossRef]
41. Berkes, C.A.; Tapscott, S.J. MyoD and the transcriptional control of myogenesis. *Semin. Cell Dev. Biol.* **2005**, *16*, 585–595. [CrossRef]
42. Jin, W.; Peng, J.; Jiang, S. The epigenetic regulation of embryonic myogenesis and adult muscle regeneration by histone methylation modification. *Biochem. Biophys. Rep.* **2016**, *6*, 209–219. [CrossRef] [PubMed]
43. De Tommasi, N.; De Simone, F.; Pizza, C.; Mahmood, N.; Moore, P.S.; Conti, C.; Orsi, N.; Stein, M.L. Constituents of *Eriobotrya japonica*. A study of their antiviral properties. *J. Nat. Prod.* **1992**, *55*, 1067–1073. [CrossRef] [PubMed]
44. Shimizu, M.; Uemitsu, N.; Shirota, M.; Matsumoto, K.; Tezuka, Y. A new triterpene ester from *Eriobotrya japonica*. *Chem. pharm. Bull.* **1996**, *44*, 2181–2182. [CrossRef]
45. Kunkel, S.D.; Suneja, M.; Ebert, S.M.; Bongers, K.S.; Fox, D.K.; Malmberg, S.E.; Alipour, F.; Shields, R.K.; Adams, C.M. mRNA expression signatures of human skeletal muscle atrophy identify a natural compound that increases muscle mass. *Cell Metab.* **2011**, *13*, 627–638. [CrossRef]
46. Noh, K.K.; Chung, K.W.; Sung, B.; Kim, M.J.; Park, C.H.; Yoon, C.; Choi, J.S.; Kim, M.K.; Kim, C.M.; Kim, N.D.; et al. Loquat (*Eriobotrya japonica*) extract prevents dexamethasone-induced muscle atrophy by inhibiting the muscle degradation pathway in Sprague Dawley rats. *Mol. Med. Rep.* **2015**, *12*, 3607–3614. [CrossRef]
47. Cho, Y.H.; Lee, S.Y.; Kim, C.M.; Kim, N.D.; Choe, S.; Lee, C.H.; Shin, J.H. Effect of loquat leaf extract on muscle strength, muscle mass, and muscle function in healthy adults: A randomized, double-blinded, and placebo-controlled trial. *Evid. Based Complement. Alternat. Med.* **2016**, *2016*, 4301621. [CrossRef]